A CENTRALIZED APPROACH FOR SHIP TARGET DETECTION AND LOCALIZATION WITH MULTI-TRANSMITTERS GNSS-BASED PASSIVE RADAR

Ilaria Nasso, Fabrizio Santi

Department of Information Engineering, Electronics and Telecommunications – Sapienza University of Rome, Italy
ilaria.nasso@uniroma1.it; fabrizio.santi@uniroma1.it

Keywords: PASSIVE MULTISTATIC RADAR, GNSS-BASED PASSIVE RADAR, SHIP DETECTION, SHIP LOCALIZATION, MARITIME SURVEILLANCE

Abstract

This work focuses on ship target detection and localization with a passive radar system exploiting multiple navigation satellites. Particularly, a centralized approach, entirely working on the Cartesian plane, is proposed to achieve a joint detection and localization of the targets. The approach can outperform conventional decentralized approaches, where individual decisions are taken at each bistatic link and, in a second stage, localization is implemented via bistatic ranges intersection. Theoretical formulations of the probability of detection and localization for both the centralized and decentralized techniques are derived in the case of target radar cross section variation among the different links, likely occurring in the system under consideration. The effectiveness of the proposed approach is tested by means of simulated analysis. Experimental results are also provided, verifying its potentiality in practical applications.

1 Introduction

In the last decades, passive radar systems based on Global Navigation Satellite Systems (GNSS) as illuminators of opportunity have acquired an increasing interest for maritime surveillance applications due to their many benefits. As passive sensors, they only include the receiving segment, thus resulting light, low cost and deployable in places where active sensors cannot be installed. Moreover, navigation satellites offer global coverage, since their signals are available even in remote areas such as open sea. Furthermore, a large number of satellites is simultaneously available, also providing a relatively high range resolution (up to 15 m, e.g. when Galileo E5a/b is used). Over the last few years, GNSS-based passive radar have been proved effective for the detection [1][2], localization [3][4][5] and imaging of ship targets [6][7].

In this research, we focus on a multistatic configuration using a single receiver and exploiting the simultaneous transmissions from multiple satellites. Usually, in such a configuration target detection and localization are achieved via decentralized approaches: peripheral detections are implemented on the individual bistatic links and then the multiple bistatic ranges are intersected via multilateration to localize the targets [4]. However, the restricted power budget provided by GNSS makes conventional techniques used for target detection not directly applicable, especially in case of targets with small radar cross section (RCS) and/or at far ranges. To increase the target observability, different approaches have been introduced considering long integration times to strengthen the signal power on each bistatic link sufficiently to allow the ship detection [2][8][9]. These strategies usually segment the long dwell time into multiple short time frames and perform a target motion compensation (TMC) to cope with the target migration experienced in the range and Doppler (RD) domain by exploiting a set of hypothesized target kinematic parameters [2]. The motion-compensated RD maps are then quadratically integrated and the target can be detected in the long-time map corresponding to the kinematic parameters closest to the actual ones.

Anyway, the exploitation of temporal diversity implies a number of issues. First, TMC are model-based procedures, usually assuming ships sailing with constant velocity over the considered integration time. If actual target kinematic deviates from the assumed model, integration losses will be experienced due to uncompensated RD migrations. Moreover, computational complexity and memory usage increase with the number of integrated frames (i.e., overall integration time) to perform the detection [2].

At the same time, decentralized approaches cannot fully benefit of the spatial diversity provided by the multi-satellites acquisitions, having a limited ability to exploit the variation of the target response among the different illumination angles to improve the detection step. Moreover, if the target power received over a particular bistatic link does not suffice to make it detected, the use of that link for the localization task is prevented and if the target is not observed over a sufficient number of links the localization task fails.

In this work, we put forward a centralized approach that can obtain in a single step the detection and localization of the ship target. Particularly, the target power received from all the bistatic links is exploited for its detection, thus potentially enhancing the detection performance with respect to decentralized methods, also providing the target location. A similar approach operating entirely in the RD domain was presented in [3]. The centralized approach here proposed operates directly in the Cartesian domain, thus providing a clear picture of the surveyed area. Such approach is an extended version of the local plane-based technique proposed for bistatic configurations in [2] and relying on long integration times. The technique here proposed aims at trading the time diversity with the space diversity, in order to overcome the shortcomings suffered by TMC procedures operating on long datastreams and realizing at the same time the localization task. Theoretical and simulated analysis show

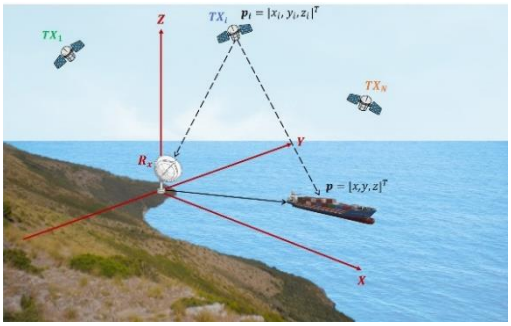

Fig 1. System geometry.

as the proposed approach can outperform conventional decentralized approaches, noticeably operating with short data frames. The effectiveness of the approach has been also tested against real data with Galileo transmitters.

The remainder of the paper is organized as follows: Section II details the operative conditions and the proposed technique, while Section III provides theoretical and simulated performance analysis; experimental results are then shown in Section IV and Section V closes the paper.

2. System overview and proposed approach

The operative conditions comprise N GNSS satellites as illuminators of opportunity and a parasitic receiver located on the coast or on a moored buoy. The receiver has two different RF channels, one collecting the direct signals from GNSS satellites in its field of view (reference channel), and one recording the signals reflections from the surveyed area (radar channel). Fig. 1 shows the right-handed (O, X, Y, Z) Cartesian reference system, centered in the receiver position and with the X-axis coinciding with the radar antenna steering direction. $\boldsymbol{p} = [x, y, z]^T$ and $\boldsymbol{p}_i = [x_i, y_i, z_i]^T$ represent respectively the target and the ith $(i = 1, \dots, N)$ satellite position. Since the focus of this work is on ship target, we can assume the motion occurring in a 2D domain: the assumed target motion model is given by x and y target position varying with constant speed $\boldsymbol{v} = [v_x, v_y, 0]^T$.

Because of the exploitation of waveforms not designed for radar purposes, ad-hoc processing schemes must be adopted to detect the ship targets of interest. First, as the signals are CW, a 2D radar reformatting according to the equivalent of fast-time and slow-time is implemented according to a fictitious Pulse Repetition Time (PRT) corresponding to the Pseudo Random Noise (PRN) primary code period (1 ms). Then, range compression is implemented by cross-correlating the radar channel data with a noise-free replica of the reference channel (achieved via synchronization algorithms, [1]) to mimic the matched filtering. Then, a Fast Fourier Transform (FFT) over the slow-time is applied thus achieving a RD map. It is worth to point out that, as the PRN codes used by GNSS are quasi-orthogonal, these operations can be implemented separately for each bistatic link. Therefore, if the overall processing gain suffices to achieve a suitable SNR, the target can be detected. Subsequently, target positioning is obtained by intersecting the bistatic ranges pertaining the different links [4]. Nevertheless, the widely separated satellites viewing angles of the target imply potentially large variations of the bistatic target RCS, resulting in a variable probability to detect it over the individual links. Consequently, the target localization may fail if the target has been not detected over a sufficient number of links (at least 2 in the considered scenario). Moreover, the system cannot fully capitalize on the possibly large RCS observed over a particular illumination angle, as only binary decisions are merged.

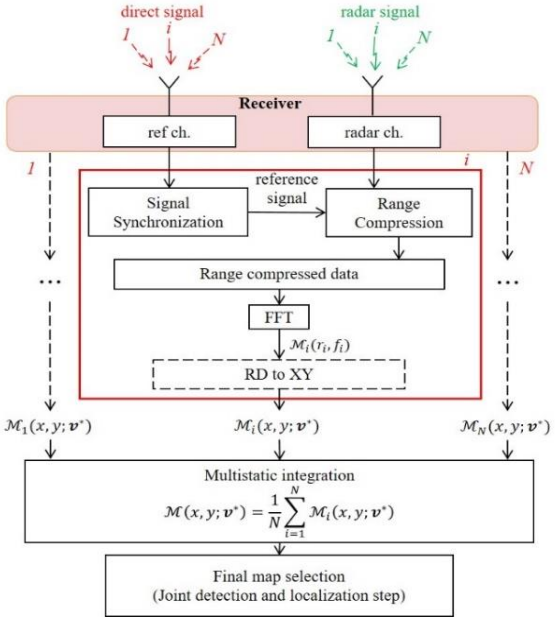

Fig. 2 Centralized approach processing chain.

Detection and localization performance can be increased by combining the received data before applying a detection threshold, i.e., by resorting to a centralized technique. If the RD maps pertaining the different bistatic links are projected over a common plane independent on the particular bistatic geometry, a multistatic integration can be nicely achieved on a pixel basis. The proposed approach is detailed in Fig. 2, and it is a modified version of the local plane-based technique proposed in [2] originally conceived for bistatic configurations and to operate over long integration times. Let $\mathcal{M}_i(r_i, f_i)$ be the RD map pertaining the ith bistatic link, where r_i and f_i denote the bistatic range and Doppler axes:

$$r_i = \|\boldsymbol{p}_i - \boldsymbol{p}\| + \|\boldsymbol{p}\| - \|\boldsymbol{p}_i\| \tag{1}$$

$$f_i = -\frac{1}{\lambda}\left(\frac{(\boldsymbol{p}_i^T - \boldsymbol{p}^T)(\boldsymbol{v}_i - \boldsymbol{v})}{\|\boldsymbol{p}_i - \boldsymbol{p}\|} + \frac{\boldsymbol{p}^T\boldsymbol{v}}{\|\boldsymbol{p}\|} - \frac{\boldsymbol{p}_i^T\boldsymbol{v}_i}{\|\boldsymbol{p}_i\|}\right) \tag{2}$$

where λ is the wavelength, $\boldsymbol{v_i}$ is the velocity vector of the ith satellite and $\|\cdot\|$ is the Euclidian norm.

Equations above show the relationship between the RD and Cartesian domains. A mapping from the RD to the Cartesian plane can be obtained by identifying for each (x, y) position corresponding to the surveyed area and for each admissible target velocity the corresponding RD cell and storing its value in a local map. Therefore, for each tested target velocity $\boldsymbol{v}^*$, a Cartesian map $\mathcal{M}_i(x, y; \boldsymbol{v}^*)$ for each link is obtained. Noticeably, target position in the ith map does not depend on the particular transmitter-receiver pair. Therefore, the maps pertaining the same tested velocity can be directly combined (in the intensity domain) thus achieving a multistatic local map:

$$\mathcal{M}(x, y; \boldsymbol{v}^*) = \frac{1}{N}\sum_{i=1}^{N} |\mathcal{M}_i(x, y; \boldsymbol{v}^*)|^2 \tag{3}$$

The multistatic map pertaining the tested velocity closest to the actual value provides the highest integration gain, so that the target can be detected. Additionally, as the signal power will be concentrated in the area occupied by the target, an estimate of the target location is directly obtained.

3 Performance Analysis

In this section, the performances of the proposed centralized approach are derived and compared with the ones achievable with decentralized strategies.

3.1 Decentralized schemes performance

Let α_i be the pixel of the ith RD map. A binary hypothesis test can be formulated as

$$\alpha_i = \begin{cases} w & , \mathcal{H}_0 \\ A_i + w & , \mathcal{H}_1 \end{cases} \quad (4)$$

Under the null hypothesis $\mathcal{H}_0$, the RD cell contains background noise only; as the system is essentially noise limited [1], this can be modeled as white Gaussian noise with power σ_w^2, i.e., $w \sim \mathcal{CN}(0, \sigma_w^2)$ (being $\mathcal{CN}$ the complex normal) and independent from the considered baselines, since the system is composed by a single receiver. Whereas under the alternative hypothesis $\mathcal{H}_1$, the received signal is composed by the noise plus the target contribution characterized by a complex amplitude A_i, modelled as a zero-mean complex random variable with variance σ_i^2, i.e., $A_i \sim \mathcal{CN}(0, \sigma_i^2)$. It is worth to point out that because of the different illumination angles, the target received power can vary among the bistatic links, i.e., σ_i^2 depends on the index i.

From (4), it is easy to obtain the probability of false alarm P_{FA}^{dec} and probability of detection $P_{D_i}^{dec}$ for the ith baseline as

$$P_{FA_i}^{dec} = P_{FA}^{dec} = e^{-T_h^{dec}/\sigma_w^2} \quad (5)$$

$$P_{D_i}^{dec} = e^{-\frac{T_h^{dec}/\sigma_w^2}{SNR_i+1}} \quad (6)$$

where T_h^{dec} is the detection threshold.

To localize the target, a detection must occur at least in $N_{min} = 2$ RD maps, so that multilateration procedures can be applied (of course, $N_{min} = 3$ would be needed if localization in 3D must be performed). Therefore, the probability of localization with a decentralized procedure is equal to the probability that at least on two bistatic links between the available N (i.e., minimum number necessary for the localization in a 2D domain) a detection takes place. Since the bistatic RD maps represent independent statistic events and are characterized each by a probability of detection $P_{D_i}^{\text{dec}}$, the probability of localization $P_{\text{L}}^{\text{dec}}$ can be computed as a cumulative Poisson binomial distribution of independent Bernoulli trials with different probabilities [10]. Particularly

$$P_{\text{L}}^{\text{dec}} = \sum_{l=N_{min}}^{N} \sum_{A \in F_l} \prod_{i \in A} P_{D_i}^{\text{dec}} \prod_{j \in A^C} (1 - P_{D_j}^{\text{dec}}) \quad (7)$$

where F_l is the set of all the subsets of l integers that can be selected from $\{2, \dots, N\}$ (e.g., for $N = 3$, $F_2 = \{(1,2), (1,3), (2,3)\}$), A represents the subsets of F_l, A^C the complement of A ($A^C = \{2, \dots, N\} \backslash A$). As a special case where all the N maps show the same SNR (i.e., $P_{D_i}^{\text{dec}} = P_D^{\text{dec}}\ \forall i$), the probability of localization of the decentralized technique simplifies to

$$P_{\text{L}}^{\text{dec}} = \sum_{j=N_{min}}^{N} \binom{N}{j} \left(P_d^{\text{dec}}\right)^j \left(1 - P_d^{\text{dec}}\right)^{N-j} \quad (8)$$

3.2 Centralized schemes performance

Let $\beta_i(\boldsymbol{v}^0)$ be the pixel of the ith local map $\mathcal{M}_i(x, y; \boldsymbol{v}^0)$, $\boldsymbol{v}^0$ being the tested velocity providing the maximum gain. A binary hypothesis test can be formulated as in (4), but in this case the detection threshold is applied after the multistatic combination (3). Let $\beta(\boldsymbol{v}^0)$ be the pixel of the multistatic map $\mathcal{M}(x, y; \boldsymbol{v}^0)$, the probability density function under the null and alternative hypothesis, $p_\beta(z; \mathcal{H}_0)$ and $p_\beta(z; \mathcal{H}_1)$, respectively, have to be evaluated to derive the corresponding probability of false alarm P_{FA}^{cen} and probability of detection P_D^{cen} of the proposed centralized scheme. In the former case, $p_\beta(z; \mathcal{H}_0)$ follows a Gamma distribution with shape parameter N and scale parameter σ_w^2 and the probability of false alarm is therefore equal to

$$P_{FA} = 1 - \gamma\left(N, {}^{T_h^{cen}}\!/_{\sigma_w^2}\right) \Big/ \Gamma(N) \quad (9)$$

where $\Gamma(\cdot)$ is the Gamma function, $\gamma(a, b) = \int_0^b t^{a-1} e^{-t} dt$ is the lower incomplete gamma function, and T_h^{cen} is the detection threshold. $p_\beta(z; \mathcal{H}_1)$ is achieved as the summation of N independent negative exponential distributions with different rate parameters [11] and it is given by (10) shown bottom to this page. The probability of detection is therefore obtained as (11) shown bottom to this page. To be noticed that (10) requires strictly distinct SNRs (where $SNR_i = \sigma_i^2/\sigma_w^2$) among the bistatic links. In the special case of $SNR_i = SNR\ \forall i$, $p_\beta(z; \mathcal{H}_1)$ follows a Gamma distribution with shape parameter N and scale parameter $\sigma_w^2(1 + SNR)$ and therefore the probability of detection simplifies to

$$P_D^{cen} = 1 - \gamma\left(N, {}^{T_h^{cen}}\!/_{\sigma_w^2(1+SNR)}\right) \Big/ \Gamma(N) \quad (12)$$

Since with the centralized approach the detection and localization of the target are joint operations, (11) and (12) also represent the centralized probability of localization P_L^{cen}.

3.3 Performance comparison

Fig. 3 shows the comparison of the performance of the decentralized (pink curves) and centralized (blue curves) approaches by varying the SNR of the bistatic links. For both the techniques, false alarm level is set to 10^{-3}. The full lines represent the theoretical performance, while the markers show

$$p_\beta(z; \mathcal{H}_1) = \prod_{i=1}^{N} \frac{1}{\sigma_w^2(1 + SNR_i)} \cdot \sum_{j=1}^{N} \frac{e^{-z/\sigma_w^2(1+SNR_j)}}{\prod_{\substack{k=1 \\ k \neq j}}^{N} \left(\frac{1}{\sigma_w^2(1 + SNR_k)} - \frac{1}{\sigma_w^2(1 + SNR_j)}\right)}, \quad SNR_j \neq SNR_k\ (j, k = 1, \dots, N) \quad (10)$$

$$P_D^{cen} = \prod_{i=1}^{N} \frac{1}{\sigma_w^2(1 + SNR_i)} \cdot \sum_{j=1}^{N} \frac{\sigma_w^2(1 + SNR_j) e^{-\frac{T_h^{cen}/\sigma_w^2}{SNR_j+1}}}{\prod_{\substack{k=1 \\ k \neq j}}^{N} \left(\frac{1}{\sigma_w^2(1 + SNR_k)} - \frac{1}{\sigma_w^2(1 + SNR_j)}\right)}, \quad SNR_j \neq SNR_k\ (j, k = 1, \dots, N) \quad (11)$$

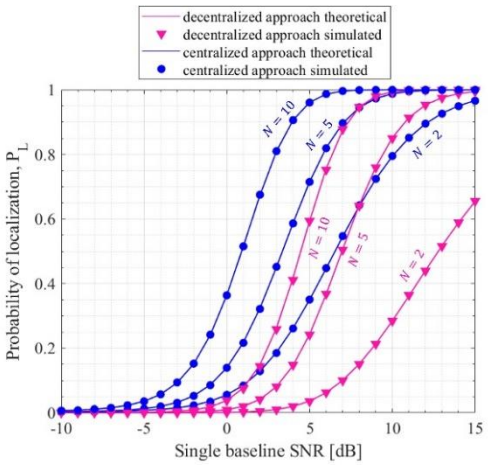

a

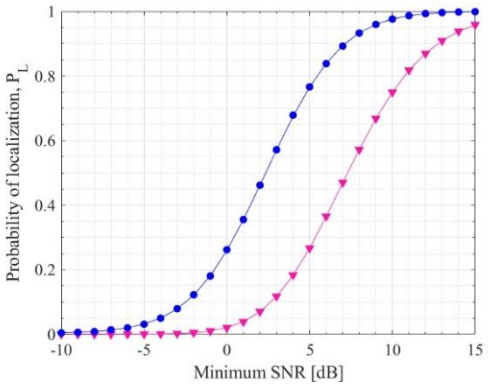

b

Fig. 3 Performance comparison: *(a)* probability of localization as a function of the number of satellites with same SNR; *(b)* probability of localization with $N = 3$ and different SNR.

the results obtained with 100000 independent Monte Carlo simulations. Fig. 3 (a) shows the comparison between the two approaches by assuming the same signal power between the bistatic links ($\sigma_i^2 = \sigma^2 \; \forall i$, i.e., same SNR) and by varying the number of satellites ($N = 2{,}5{,}10$). It can be noticed as the localization performance of both the techniques gradually improve by increasing the number of satellites. Particularly, by observing curves with same number of bistatic links, the exploitation of the centralized approach brings an enhancement in the localization task. E.g., for $N = 2$ and $SNR = 12$ dB, the decentralized approach provides a probability of localization equal to 45%, while the proposed scheme achieves $P_L \approx 90\%$. Fig. 3 (b) shows a case of SNR varying among the links. Particularly, the figure shows the localization probability as a function of the minimum SNR among $N = 3$ available links, by setting $SNR_1 = SNR_{min}$, $SNR_2 = SNR_1 + 2$ dB and $SNR_3 = SNR_1 + 5$ dB. In this case study, the proposed scheme can achieve a probability of localization of 90% with about 6 dB lower SNR_{min} than in the conventional decentralized approach.

4 Experimental Results

The proposed approach has been tested against real data collected during an acquisition campaign in Porto Marghera (Italy). The receiver was placed at the entrance of the port, with the radar antenna pointed toward the terminal area, collecting signals emitted by Galileo satellite in E5a band (carrier frequency: 1176.45 MHz, bandwidth: 10.23 MHz)

a

b

Fig. 4 *(a)* acquisition geometry: *(b)* photograph of the target of opportunity (source: [12]).

Table 1 Tracked satellites

Parameter		Unit	Value
Satellite 1	Number	-	GSAT0207
	Ranging code	-	E07 (E5a-Q)
	Azimuth* angle	deg	-51.83~-51.14
	Elevation** angle	deg	65.84~66.84
Satellite 2	Number	-	GSAT0211
	Ranging code	-	E02 (E5a-Q)
	Azimuth angle	deg	67.91~66.84
	Elevation angle	deg	48.67~49.23
Satellite 3	Number	-	GSAT0208
	Ranging code	-	E08 (E5a-Q)
	Azimuth angle	deg	102.12~103.46
	Elevation angle	deg	56.15~55.26

* calculated clockwise from *X*-axis
** evaluated from receiver position

and scattered by commercial vessels entering/exiting the port [Fig. 4 (a)]. The Automatic Identification System (AIS) messages were also recorded to be used as ground truth. During the acquisition, the cargo Fairpartner [Fig. 4 (b), size 143.1 m × 26.6 m] was entering in the port terminal and three Galileo satellites signals were collected: GSAT0207, GSAT0211 and GSAT208, using PRN codes E07, E02, and E08, respectively (hereinafter denoted as sat.1, sat. 2 and sat. 3). Table 1 lists the parameters of the tracked satellites. A coherent processing interval of 3 s has been used, achieving for each time instant a RD map for each bistatic link.

Fig. 5 shows the individual bistatic RD maps for the three baselines corresponding to the time interval at the beginning of the acquisition. The white squares highlight the RD positions of the target as calculated from the AIS and, as it is apparent, the received target power considerably varies among the links: the target is barely visible with sat. 1 and sat. 2 and it is completely buried in the noise background with sat. 3. The

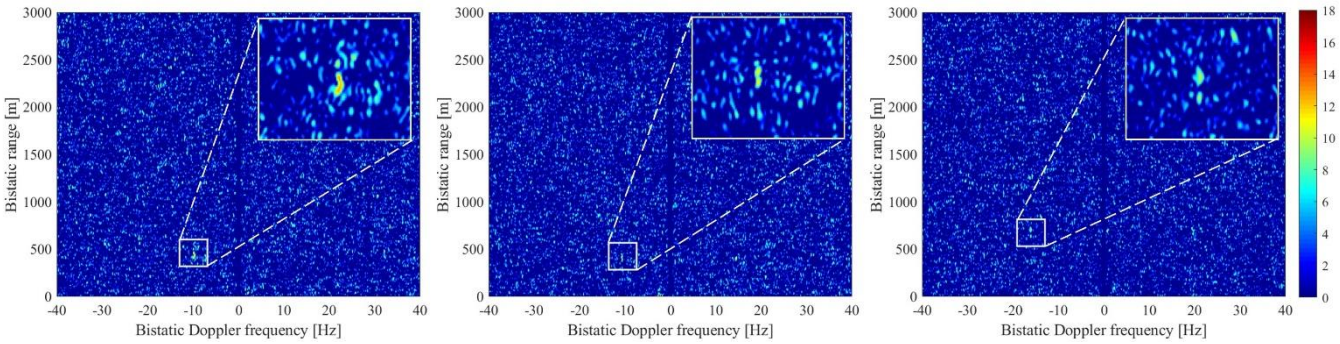

a *b* *c*

Fig. 5 Fairpartner bistatic RD maps *(a)* sat. 1; *(b)* sat. 2; *(c)* sat. 3.

Table 2 Experimental Probability of Detection and Localization

P_{fa}	P_{D_1}	P_{D_2}	P_{D_3}	P_L^{dec}	P_L^{cen}
10^{-3}	69.89%	62.06%	51.34%	66.58%	95.50%
10^{-4}	62.02%	52.94%	41.11%	53.10%	92.51%

low levels of SNR observed with these satellites can lead to detection performance degradation when using decentralized approaches and, consequently, also in localization.

The probabilities to detect the target in the individual links are listed in Table 2 (using the SNR level evaluated from the maps) with the corresponding P_L^{dec}. The probabilities to localize the target are not high, well below typical operative requirements for maritime surveillance applications, due to the high missed detection rates in the individual links.

Fig. 6 shows the local map obtained with the proposed centralized approach providing the maximum gain among all the tested velocities. As it is apparent, the target contributions as observed among the links integrate over the same area in the Cartesian plane, allowing a higher probability to detect it and therefore to localize it. Particularly, a probability of localization over 90% can be achieved in this case study for both P_{FA} equal to 10^{-3} and 10^{-4}, about 29% and 39% greater, respectively, than the decentralized scheme (see Table 2).

Fig. 7 shows the Fairpartner position estimations using the decentralized and centralized techniques [Fig. 7 (a) and Fig. 7 (b), respectively] for 21 different time instants, shifting each time the integration window of 5 s starting from the beginning of the acquisition. The full lines are the AIS positions, while red '×' markers denote the estimated positions. (In the centralized case, position estimate is evaluated as central position of the cluster of pixels in the binary map.) As with the decentralized approach the localization requires the target to be detected at least on 2-out-of-3 bistatic maps, a number of missed localizations occur, denoted as black '□' markers in the figure. Significant errors can also be observed in few time instants, which might be because the target has been detected only on 2 bistatic links with relatively similar bistatic geometries. Moreover, the large target size and the variation of the e.m. response over the channels might entail the intersection of ranges pertaining different scattering centers.

Table 3 lists the successful (✓) and missed (×) localizations in the different time instants, while numerical results are reported in Table 4. With the conventional decentralized

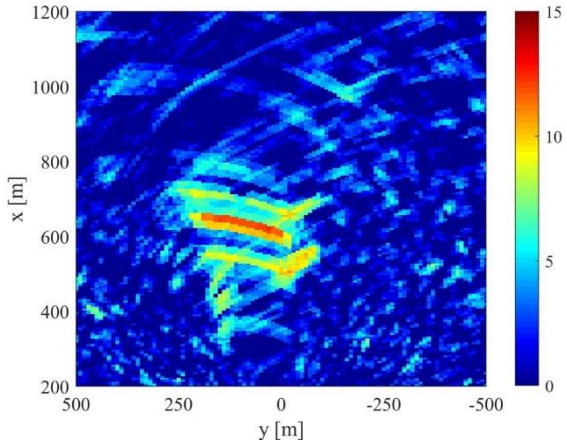

Fig. 6 Experimental local map.

approach, the localization task fails 9/21 times, corresponding to an estimated $\hat{P}_L^{dec}$ of about 57%. In contrast, reinforcing the received signal power by means of the exploitation of the multiple illumination angles with the proposed method allowed providing a position estimate for each considered time instant.

Finally, last column of Table 4 lists the Root Mean Square (RMS) errors of the estimates achieved with the two approaches, evaluated taking the AIS as reference. It can be observed as the proposed scheme also allowed an improvement in the accuracy of the position estimate, because of the higher SNR of the multistatic map.

5 Conclusion

This work addressed the detection and localization of ship targets with a multistatic passive radar system based on GNSS illuminators. Particularly, the proposed method achieves a joint detection and localization of the target in a single step, so capitalizing on the spatial diversity offered by navigation satellites to overcome the limitations due to the restricted power budget. As it operates entirely in the Cartesian plane, the technique directly provides a picture of the surveyed area. Noticeably, not any compensation of the target range and Doppler migration is needed, which is a remarkable benefit in terms of robustness of the signal integration against model mismatches. However, the approach could be extended to the case of multi-frame (i.e., requiring TMC strategies) and multistatic integration, potentially carrying to enhanced performance. It is worth mentioning that, even though it generally requires a heavier computational load than decentralized strategies, as in the considered multistatic

Table 3 Localization results for different timestamps

Time stamp	1	5	10	15	20	25	30	35	40	45	50	55	60	65	70	75	80	85	90	95	100
Decentralized approach	✓	✓	✓	×	✓	×	✓	×	✓	×	✓	✓	✓	×	✓	×	×	✓	✓	×	×
Centralized approach	✓	✓	✓	✓	✓	✓	✓	✓	✓	✓	✓	✓	✓	✓	✓	✓	✓	✓	✓	✓	✓

Table 4 Numerical results

Approach	*Localizations*	$\widehat{P}_L$	RMS error
Decentralized	12/21	57.14%	143.09 m
Centralized	21/21	100%	40.34 m

configuration the single receiver acts as collector of the multichannel data, setting a broadband communication channel is not required.

Performance improvements with respect to the conventional approaches operating in two separated stages for detecting and localizing the target have been theoretically evaluated and analyzed by means of simulations. Moreover, the effectiveness of the method has been tested against experimental data set, validating its potentialities to outperform decentralized approaches in practical applications.

6 Acknowledgements

The experimental campaigns were carried out inside the research project "GALILEO-BASED PASSIVE RADAR SYSTEM FOR MARITIME SURVEILLANCE—SpyGLASS" funded from the European GNSS Agency under the European Union's Horizon 2020 research and innovation programme under grant agreement No. 641486.

7 References

[1] Ma, H., Antoniou, M., Pastina, D., *et al.*, 'Maritime moving target indication using passive GNSS-based bistatic radar', *IEEE Trans. Aero. Elect. Syst.*, 2018, 54, (1), pp. 115-130.

[2] Pastina, D., Santi, F., Pieralice, F., *et al.*, 'Maritime moving target long time integration for GNSS-based passive bistatic radar', *IEEE Trans. Aero. Elect. Syst.*, 2018, 54, (6), pp. 3060-3083.

[3] Santi, F., Pieralice, F., Pastina, D., 'Joint detection and localization of vessels at sea with a GNSS-based multistatic radar', *IEEE Trans. Geosci. Remote Sens.*, 2019, 57, (8), pp. 5894-5913.

[4] Ma, H., Antoniou, M., Stove, A.G., Winkel, J., Cherniakov, M., 'Maritime moving target localization using passive GNSS-based multistatic radar', *IEEE Trans. Geosci. Remote Sens.*, 2018, 56, (8), pp. 4808-4819.

[5] Sadeghi, M., Behnia, F., Amiri, R., 'Maritime target localization from bistatic range measurements in space-based passive radar', *IEEE Trans. Instrum. Meas.*, 2021, 70, pp. 1-8.

[6] Pastina, D., Santi, F., Pieralice, F., Antoniou, M., Cherniakov, M., 'Passive Radar Imaging of Ship Targets With GNSS Signals of Opportunity', 2021, *IEEE Trans. Geosci. Remote Sens.*, 59, (3), pp. 2627-2642.

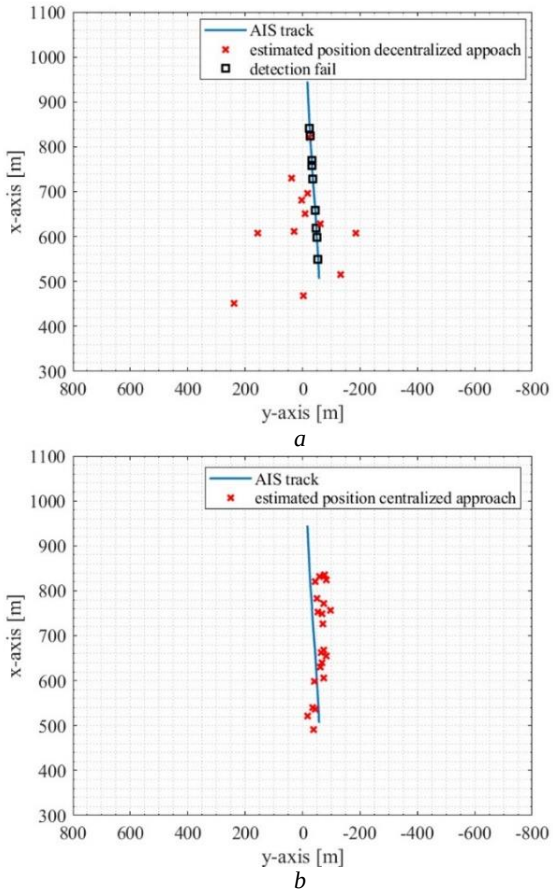

Fig. 7 Estimated target position: *(a)* decentralized approach; *(b)* centralized approach.

[7] Santi, F., Pastina, D., Antoniou, M., Cherniakov, M., 'GNSS-based multistatic passive radar imaging of ship targets', *IEEE Int. RadarConf.*, Apr. 2020, pp. 601-606.

[8] Huang, C., Li, Z., Lou, M., *et al*., 'BeiDou-Based Passive Radar Vessel Target Detection: Method and Experiment via Long-Time Optimized Integration', *Remote Sensing*, 2021, 13, (19), 3933.

[9] Z. He, Y. Yang, and W. Chen, 'A hybrid integration method for moving target detection with GNSS-based passive radar,' *IEEE J. Sel. Topics Appl. Earth Observ. Remote Sens.*, vol. 14, pp. 1184-1193, Jan. 2021.

[10] Wang, Y. H. 'On the number of successes in independent trials', *Stat. Sinica*, 1993, 3, (2), pp. 295-312.

[11] Levy, E., 'On the density for sums of independent exponential, Erlang and gamma variates', *Stat. Papers*, 2021, 1-29.

[12] 'Marine Traffic'. [Online]. Available: https://www.marinetraffic.com.